α- and 3_{10}-Helix Interconversion: A Quantum-Chemical Study on Polyalanine Systems in the Gas Phase and in Aqueous Solvent

Igor A. Topol,[†] Stanley K. Burt,[†] Eugen Deretey,[‡] Ting-Hua Tang,[‡] Andras Perczel,[§] Alexander Rashin,[⊥] and Imre G. Csizmadia[‡]

Advanced Biomedical Computing Center, SAIC Frederick, P.O. Box B, National Cancer Institute at Frederick, Frederick, Maryland 21702-1201; Department of Chemistry, University of Toronto, Toronto, Ontario, Canada, M5S 3H6; Institute of Organic Chemistry, Eotvos University, 112 Budapest, P.O. Box 32 2 Pazmany Peter setany, H-1117, Hungary; and BioChemComp, Inc., 543 Sagamore Avenue, Teaneck, New Jersey 07666

Received November 7, 2000. Revised Manuscript Received April 30, 2001

Abstract: Helices are among the predominant secondary structures in globular proteins. About 90% of the residues in them are found to be in the α-helical conformation, and another 10% in the 3_{10} conformation. There is a standing controversy between experimental and some theoretical results, and controversy among theoretical results concerning the predominance of each conformation, in particular, helices. We address this controversy by ab initio Hartree−Fock and density functional theory studies of helices with different lengths in a vacuum and in the aqueous phase. Our results show that (1) in a vacuum, all oligo(Ala) helices of 4−10 residues adopt the 3_{10} − conformation; (2) in aqueous solution, the 6−10 residue peptides adopt the α-helical conformation; (3) there might be two intermediates between these helical conformers allowing for their interconversion. The relevance of these results to the structure and folding of proteins is discussed.

1. Introduction

Three types of right-handed helices occur in proteins: 3_{10}, 4_{13} (or α helix), and 5_{16} (or π helix). The symbols 3_{10}, 4_{13}, and 5_{16} imply that the intramolecular hydrogen bonds form a ring containing 3, 4, or 5 sequential carbonyl oxygens and consisting of 10, 13, or 16 atoms, respectively. These helices, for a given length of oligo- or polypeptide, have different numbers of hydrogen bonds between the CO of residue *n* and the NH of residue $n + 3$, $n + 4$, or $n + 5$ counting from the N-terminus of the olygopeptide, as shown in Figure 1. For the same number of amino acid residues, the 3_{10} helix has the most number of hydrogen bonds, and the 5_{16} helix has the least. Consequently, the 3_{10} helix is expected to be the most stable, and the 5_{16} helix is expected to be the least stable. It is not surprising, therefore, that π helices are hardly ever observed. Even though a 3_{10} helix has one more hydrogen bond than the 4_{13} or α helix, it is the α helix that dominates in protein structures; nevertheless, about 10% of helical structures[1] in proteins are 3_{10} helices. However, despite the fact that both helices have been observed, it is not clearly understood which factors are favoring the formation of each helix type[2].

In fact, early empirical calculations of helical structures predicted that the 3_{10} helix is outside the range of stability, but the α helix is in a minimum.[3,4] This, however, might have been an artifact of the empirical potentials developed to reproduce

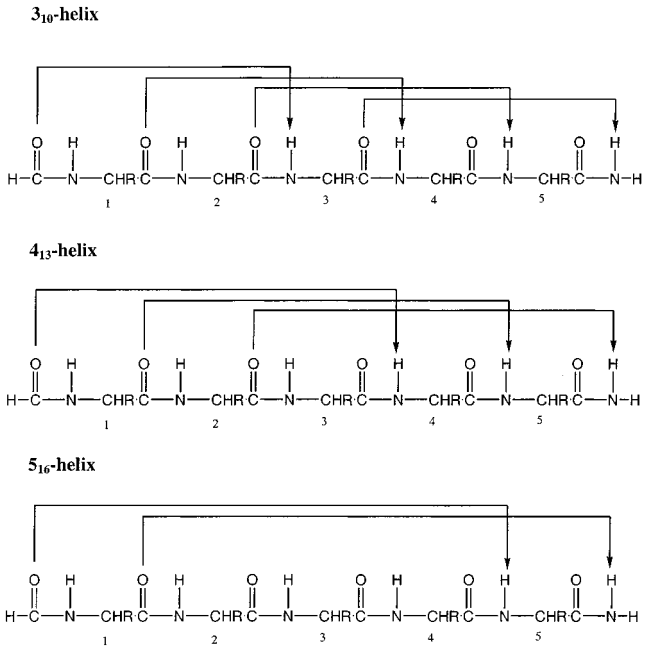

Figure 1. Schematic 2-D representation of the three helical conformations. Arrow lines denote hydrogen bonds.

conformational preferences in proteins**.** It has been repeatedly noted that in the α helix, hydrogen bonds are almost parallel to the helix axis, but are quite tilted in the 3_{10} helices, and that both the hydrogen bond geometry and van der Waals interactions between the successive turns are not as favorable in the 3_{10} helices as in the α helices. It has also been suggested from protein structure observations that the major importance of the 3_{10} helix is that it very frequently forms the last turn at the C-terminus of an α helix.[5]

[†] National Cancer Institute at Frederick. E-mails: topol@ncifcrf.gov; burt@ncifcrf.gov.

[‡] University of Toronto. E-mails: ederetey@alchemy.chem.utoronto.ca; ttang@alchemy.chem.utoronto.ca; icsizmad@alchemy.chem.utoronto.ca.

[§] Eotvos University. E-mails: aperczel@biotech.ox.ac.uk; perczel@szerves.chem.elte.hu.

[⊥] BioChemComp, Inc. E-mail: rashin@idt.net.

(1) Barlow, D. J.; Thornton, J. M. *J. Mol. Biol.* **1988**, *201*, 601.
(2) Millhauser, G. L. *Biochemistry* **1995**, *34*, 3874.
(3) Scheraga, H. A. *Adv. Phys. Org. Chem.* **1968**, *6*, 103.
(4) Brant, D. A. *Macromolecules*, **1968**, *1*, 291.

10.1021/ja0038934 CCC: $20.00
Published on Web 05/26/2001

The formation of α helices is traditionally described by the Zimm-Bragg theory[6] or its modified forms.[7,8] In these theories, the probability (equilibrium constant) of finding a particular sequence in the helical conformation is determined by the product of the nucleation constant σ (usually of the order of 10^{-4}) and propagation constants s for each residue (usually between slightly less than 1 and 1.3), and it has been shown that unusually high stabilities of helices can be influenced by sequence. The small value of the initiation constant probably results from the need to simultaneously fix at least four contiguous residues in the helical conformation to form the first hydrogen bond of the α helix. As a result, even with the maximum observed value of $s = 1.3$, a 13-residue peptide would be expected to be helical only 8% of the time.[9] The finding of short oligopeptides with helicities of up to 50%, prompted restudying of σ and s as well as an introduction of side-chain interactions into the theories. Despite the accumulation of experimental results and theoretical modifications, the values of the constants as well as the theoretical interpretations remain somewhat uncertain.[10−12]

It should be noted that the initiation of the 3_{10} helix requires the fixation of three residues, or one less than for the α helices. Thus, the nucleation constant, σ_{3_10}, for the 3_{10} helix can be an order of magnitude larger than that of σ_α associated with the α helix. Together with one more H bond in the 3_{10} helix than in the α helix, this might make the 3_{10} helices more stable among the two helical conformations, despite the better geometry of the H bonds and van der Waals interaction in the α helix. In other words, if we denote the number of the hydrogen bonds in the α helix as n, the product $\sigma_{3_10}s_{3_10}{}^{n+1}$can be larger than $\sigma_\alpha s_\alpha{}^n$ for some n, despite the fact that $s_{3\_10} < s_\alpha$; however, for a sufficiently large n, the product will become larger for the α helix. Alternatively, one may argue that both helices lose the same amount of entropy in their folding, and thus, the entire advantage of the 3_{10} helix is one extra hydrogen bond that is somewhat weaker than in the α helix. In this interpretation, for a sufficiently large n, the accumulated strength of the α-helical H bonds overrides the advantage of the extra H bond in the 3_{10} helix.

The first findings of oligopeptides in the 3_{10} conformation were reported for peptides containing Aib (Aib is α-aminoisobutiric acid), which is a branched amino acid found in some natural microbial antibiotics.[13−15] In Aib, there are two methyl groups bonded to the C_α atom, in contrast to the presence of a methyl group and H in alanine. This imposes additional restriction on the conformational freedom in Aib as compared to most natural amino acid residues. It has been found that depending on Aib content, length, and the crystal or solvent interactions, these peptides adopt 3_{10} conformation for shorter lengths and mixed $\alpha/3_{10}$ conformation for longer peptides (e.g., 8-mers). Therefore, the nonnatural amino acid peptides lend further indications[13−15,19] that the $\alpha/3_{10}$ helix equilibrium can be significant in understanding the conformation of helices.

Experimental ESR data published in 1992 for the first time strongly indicated that 16-residue-long Ala-based peptides form a 3_{10} rather than the expected α helix in solution.[16] Hanson et al.[17] found later for a 16-residue-long sequence in methanol, that this peptide adopts a more "open geometry than α helix, having approximately 3.8−3.9 residues per turn-units". Other experimental studies confirmed 3_{10} helix conformation in the entire 16-mer, but in the 21-mer, it found α helix conformation up to residue 13 and 3_{10} helix in the remaining C-terminal residues.[17] Recent experimental ESR studies of Ala-based peptides showed preferred α-helical structures and restored the common point of view that α helices are dominant in water.[18] In studying solvent effects, using organic−aqueous solvent mixtures, it was found[20] that the 3_{10}- → α-helix conversion was enhanced as the water content increased from 0 to 50%. Furthermore, using solid-state NMR data, Long and Tycko[21] observed for a 17-mer-long helical peptide that addition of urea has an intrinsic effect on converting α- into 3_{10}-helical conformation. They proposed that 3_{10}-helical units could be thermodynamic intermediates during α-helix folding and unfolding in peptides and proteins. Recently, high-field NMR studies of the alanine-rich peptides in solution[22] showed nuclear Overhauser effect (NOE) patterns, suggesting that there is a significant amount of 3_{10} helix in the investigated moiety. They determined explicitly the ratio of 3_{10} and α helix by integrating the NOE intensities and found that whereas the core region of the secondary structural element is dominated by a-helical conformation, a nearly equal proportion of two helical forms occurs at both ends. Most of these experimental studies concluded that helical peptides are plastic structures and could be in rapid interconversion of a wide range of helix-like conformers as a function of their molecular environment.

The stability of α-helical conformations vs 3_{10} conformations of polypeptides has been the subject of numerous molecular simulations. Molecular dynamics calculations seem to show that decaalanine is preferably α-helical in both vacuum and solution (for a review, see ref 23). In particular, the decamethylalanine α helix has been found to be 3.3 kcal/mol more stable than the 3_{10} helix in a vacuum and 8 kcal/mol more stable in solution, and it has been indicated that this difference might be even larger in the decaalanine.[24] Other molecular dynamics simulations for decaalanine showed that this polypeptide prefers the α helix over the 3_{10} helix by 16 kcal/mol in water, and 8.0 kcal/mol in vacuo, but Aib_{10} showed no clear preference in water and prefers the 3_{10} helix by 4.3 kcal/mol in vacuo.[25] The molecular dynamics

(5) Richardson, J. S.; Richardson, D. C. In *Prediction of Protein Structure and the Principles of Protein Conformation*; Fastman, G. D., Ed.; Plenum Press: New York, **1989**, pp 1−98.
(6) Zimm, B. H.; Bragg, J. K. *J. Chem. Phys.* **1959**, *31*, 526.
(7) Vasques. M.; Scheraga, H. A. *Biopolymers* **1988**, *27*, 41.
(8) Finkelstein, A. V.; Badretdinov, A. Y.; Ptitsyn, O. B. *Proteins* **1991**, *10*, 287.
(9) Creighton, T. E. *Nature*, **1987**, *326*, 547.
(10) Kemp, D. S.; Boyd, J. G.; Muendel, C. C. *Nature* **1991**, *352*, 451.
(11) Scholtz, M.; Baldwin, R. L. *Annu. Rev. Biophys. Biomol. Struct.* **1992**, *21*, 95.
(12) Rashin, A. A. *Proteins* **1992**, *13*, 120.
(13) Paterson, Y.; Stimson, E. R.; Evans, D. J.; Leach, S. J.; Scheraga, H. A. *Int. J. Peptide Protein Res.* **1982**, *20*, 468.
(14) Marshall, G. R.; Hodgkin, E. E.; Langs, D. A.; Smith, G. D.; Zabrovski, J.; Leplawy, M. L. *Proc. Natl. Acad. Sci. U.S.A.* **1990**, *87*, 487.
(15) Pavone, V.; Benedetti, E.; Di Blasio, B.; Pedone, C.; Santini, A.; Bavoso, A.; Toniolo, C.; Crisma, M.; Sartore, L. *J. Biomol. Struct. Dyn.* **1990**, *7*, 1321.
(16) Miick, S. M.; Martinez, G. V.; Fiori, W. R.; Todd, A. P.; Millhauser, G. L. *Nature*, **1992**, *359*, 653.
(17) Hanson, P.; Anderson, D. J.; Mertinez, G.; Millhauser, G.; Formaggio, F.; Crisma, M.; Toniolo, C.; Vita, C. *Mol. Phys.* **1998,** *95*, 957.
(18) Fiori, W. R.; Miick, S. M.; Millhauser, G. L. *Biochemistry* **1993**, *32*, 11957.
(19) Smythe, M. L.; Nakaie, C. R.; Marshall, G. R. *J. Am. Chem. Soc.* **1995**, *117*, 10555.
(20) Yokum, T. S.; Gauthier, T. J.; Hammer, R. P.; McLaughlin, M. L. *J. Am. Chem. Soc.* **1997**, *119*, 1167.
(21) Long, H. W.; Tycko, R. *J. Am. Chem. Soc.* **1998**, *120*, 7039.
(22) Millhauser, G. L.; Stenlad, C. J.; Hanson, P.; Bolin, K. A.; Van de Ven, J. M. *J. Mol. Biol.* **1997**, *267*, 963.
(23) Vasques, M.; Nemethy, G.; Scheraga, H. A. *Chem. Rev.* **1994**, *94*, 2184.
(24) Smythe, M. L.; Huston, S. E.; Marshall, G. R. *J. Am. Chem. Soc.* **1993**, *115*, 1993, 11594.
(25) Zhang, L.; Hermans, J. *J. Am. Chem. Soc.* **1994**, *116*, 11915.

and Monte Carlo simulations by Jorgensen et al.[26] conducted for undecaalanine demonstrated that the α-helical form is intrinsically much more stable than the 3_{10} alternative, and whether or not the solvent was taken into account, the preference was preserved. Sheinerman and Brooks[27] used the modified Zimm−Bragg theory and found that 3_{10} helices are, on average, shorter than α helices and can be thermodynamic intermediates of α-helix formation. Using -AAAK- repeats[28] and other helical peptides[29] as models for molecular dynamics simulations, it has been shown that 16-mer alanine-rich peptides samples dominating helical conformation in the cases of both CHARMM22 and AMBER95 force field usage. As mentioned above, the discrepancy between molecular simulations and some of the observations could be an artifact of the empirical potentials that are used.

Previous quantum chemical computational studies of helices involved PCO-NH-$(Ala)_n$-CO-NHQ (where P and Q may be H or Me) for up to a tetrapeptide[30] (i.e., $n = 4$) and a pentapeptide[31] ($n = 5$). Both of these studies[30,31] reported 3_{10} helices rather than α helices as ground-state structures.

Thus, there is a standing controversy between the experimental and some theoretical results, and among theoretical results concerning conformational predominance in particular helices. Here we address this controversy by ab initio Hartree−Fock (HF) and density functional theory (DFT) studies of α and 3_{10} polyalanine helices having different lengths both in a vacuum and in the aqueous phase.

2. Computational Method

The extent of any computational study is dependent on the size of the molecule. Although reliable results can be obtained only at high levels of theory, large systems can only be studied quantum mechanically at a lower level of theory. It has been shown recently[32] that the HF/3-21G calculations, however fortuitously, give comparable results to those obtained at the MP2/6-311++G** level of theory for the intrinsic stabilities in the gaseous phase without environmental effects. We have wished to calibrate the HF/3-21G helix results with those obtained at the much higher B3LYP/6-31G* level of theory for potential use of this level of approximation for much larger polypeptides. It would be important to know if such lower level ab initio computations can give at least semiquantitative results in comparison to those of the DFT optimized parameters.

As was mentioned above, two standard Gaussian basis sets, 3-21G and 6-31G*, were used in the calculations. Both basis sets were employed to carry out Hartree−Fock type calculations (HF/3-21G and HF/6-31G*), and the latter one was used to carry out density functional calculations using the B3LYP approach (B3LYP/6-31G*).[33,34] All of the calculations were performed using parallel versions of Gaussian 94[35] and Jaguar[36] program suits at the Advanced Biomedical Computing Center on the J90 and Origin 2000 computers. Typically, 4−6 processors were used for these calculations. Solvation calculations were performed with a self-consistent reaction field method using a Poisson−Boltzmann solver, as incorporated in Jaguar.[36−38]

Table 1. Stabilities of the α Helix Relative to the 3_{10} Helix for Different Polyalanine Helix Lengths in the Gas Phase and in Aqueous Solvent[a]

	stability of α- relative to the 3_{10} helix (kcal/mol)			
helix length	$n = 4$	$n = 6$	$n = 8$	$n = 10$
medium = gas	0.11	6.30	6.49	4.87
medium = water	0.51	−11.24	−14.94	−10.36

[a] All optimizations for HCO-$(Ala)_n$-NH_2 were performed at the B3LYP/6-31G* level.

To locate certain minimums, a portion of the molecule had to be initially constrained. After the completion of the constrained optimization, the frozen geometrical parameters were gradually deconstrained, leading to fully relaxed structures. In the final structures all gradients were less than 4.5×10^{-4} a.u.

Contributions to the free energy of the helical conformations arising from vibrational contributions to the enthalpy and entropy as well as from the rotation-isomeric conformational entropy were not considered in our calculations. Torsional angles are given according to the IUPAC−IUB convention[39] within −180° and +180°.

3. Results and Discussion

A fairly large ab initio and DFT database has been compiled in this study for HCO-NH-$(Ala)_n$-$CONH_2$ systems for $n = 4$, 6, 8, and 10. The first important question we attempted to elucidate concerned relative stabilities of the two helical conformations. Data in Table 1 show the calculated stability of the α helix relative to the 3_{10} helix for all helix lengths studied. For $n = 4$, our computations show that both helices are almost equally stable within the accuracy of calculations in both a vacuum and water. However, as shown in Table 2, for $n = 4$ the optimizations starting from both ideal helical forms converge to almost the same structure as judged by their dihedral angles. This explains the similarity of their stabilities. For $n = 6$, 8, and 10, the 3_{10} helices are more stable than the α helices by 6.5−4.9 kcal/mol in a vacuum, and less stable by 10.4−15 kcal/mol in water. For all of these helix lengths, the dihedral angles remain sufficiently different between the two helical forms, preserving their hydrogen bonding patterns after the optimization, as shown for $n = 8$ in Table 3. It can be noted, however, that the optimized dihedral angles significantly deviate from their ideal values for the α ($\varphi = -55°$, $\psi = -45°$) and the 3_{10} helix ($\varphi = -60°$, $\psi = -30°$).

Thus, our results differ from those obtained from the molecular dynamics calculations[23,24] and partly from some experiments.[16,18] In contrast to the molecular dynamics and Monte Carlo simulations,[25,26] our results show the 3_{10} helix to be significantly more stable than the α helix is in a vacuum. Although some experimental data suggested a different conclusion,[16,18] we find the α helix much favored in water. The value

(26) Tirada-Rives, J.; Maxwell, D. X.; Jorgensen, W. L. *J. Am. Chem. Soc*. **1993**, *115*, 11590.
(27) Sheinerman, F. B.; Brooks, III C. L. *J. Am. Chem. Soc.* **1995**, *117*, 10098.
(28) Samuelson, S.; Martyna, G. J. *J. Phys. Chem. B.* **1999**, *103*, 1752.
(29) Bartels, C.; Schafer, M.; Karplus, M. *J. Chem. Phys.* **1999**, *111*, 8048.
(30) Endrédi, G.; McAllister, M. A.; Perczel, A.; Császár, P.; Ladik, J.; Csizmadia, I. G. *J. Mol. Struct. (THEOCHEM)* **1995**, *331*, 5.
(31) Schafer, L.; Newton, S. Q.; Cao, M.; van Alsenoy, G.; Wolinski, K.; Momany, F. A. *J. Am. Chem. Soc.* **1993**, *115*, 272.
(32) Endrédi, G.; Perczel, A.; Farkas, Ö.; McAllister, M. A.; Csonka, G. I.; Ladik, J.; Csizmadia, I. G. *J. Mol. Struct. (THEOCHEM)* **1997**, *391*, 15.
(33) Becke, A. D. *J. Chem. Phys.* **1993**, *98*, 5648.
(34) Lee, C.; Yang, W.; Parr, R. G. *Phys. Rev. B* **1988**, *37*, 785.
(35) Frisch, M. J.; Trucks, G.W.; Schlegel, H. B.; Gill, P. M. W.; Johnson, B. G.; Robb, M. A.; Cheeseman, J. R.; Keith, T.; Petersson, G. A.; Montgomery, J. A.; Raghavachari, K.; Al-Laham, M. A.; Zakrzewski, V. G.; Ortiz, J. V.; Foresman, J. B.; Cioslowski, J.; Stefanov, B. B.; Nanayakkara, A.; Challacombe, M,; Peng, C. Y.; Ayala, P. Y.; Chen, W.; Wong, M. W.; Andres, J. L.; Replogle, E. S.; Gomperts, R.; Martin, R. L.; Fox, D. J.; Binkley, J. S.; Defrees, D. J.; Baker, J.; Stewart, J. P.; Head-Gordon, M.; Gonzalez, C.; Pople, J. A. *Gaussian 94*, Revision D.4; Gaussian, Inc.: Pittsburgh, PA, 1995.
(36) Jaguar 3.5; Schroedinger, Inc.: Portland, OR, 1998.
(37) Tannor, D. J.; Marten. B.; Murphy, R.; Friesner, R. A.; Sitkoff, D.; Nicholls, A.; Ringnalda, M.; Goddard, W. A., III.; Honig, B. *J. Am. Chem. Soc*. **1994**, *116*, 11875.
(38) Marten, B.; Kim, K.; Cortis, C.; Friesner, R. A.; Murphy, R. B.; Ringnalda, M. N.; Sitkoff, D.; Honig, B. *J. Phys. Chem*. **1996**, *100*, 11775.
(39) IUPAC−IUB, Commission on Biochemical Nomenclature. *Arch. Biochem. Biophys*. **1971**, *145*, 405.

Table 2. Multiple Conformers for HCO-$(Ala)_4$-NH_2 Optimized at the B3LYP/6-31G* Level in the Gas Phase and in Aqueous Solvent and the Geometry Parameters of the Backbone

	gas phase			water		
	conf_1[a]	conf_2[b]	conf_3[c]	conf_4[a]	conf_5[b]	conf_6[c]
ω_0	−168.0	−168.1	−167.5	−172.9	−171.5	−172.1
φ_1	−66.2	−65.7	−65.6	−61.4	−60.6	−61.8
ψ_1	−22.4	−22.7	−22.0	−24.7	−26.5	−25.5
ω_1	177.7	177.9	177.5	178.2	178.01	177.6
φ_2	−62.5	−62.7	−62.5	−58.6	−58.9	−59.4
ψ_2	−19.8	−19.0	−18.7	−22.3	−21.5	−19.7
ω_2	177.0	176.8	176.8	177.7	177.1	176.9
φ_3	−71.0	−68.8	−67.3	−65.0	−63.9	−63.5
ψ_3	−7.2	−10.1	−12.1	−15.1	−16.2	−17.2
ω_3	172.9	173.8	174.2	175.1	175.7	175.5
φ_4	−103.8	−98.9	−95.1	−93.6	−92.8	−89.2
ψ_4	11.5	8.6	4.6	5.8	5.3	3.5
ω_4	176.8	177.0	174.0	177.6	177.5	177.0
energy, a.u.	−1159.2084	−1159.2082	−1159.2081	−1159.3306	−1159.3321	−1159.3329
relative energy, kcal/mol	−0.20	−0.09	0.00	1.40	0.51	0.00

[a] This structure was initially a 3_{10} helix. [b] This structure was initially a genuine 4_{13} helix. [c] This structure was initially a genuine 3_{10} helix.

of the relative stability of the α vs the 3_{10} conformation of decaalanine (−10.4 kcal/mol) obtained in the B3LYP/6-31G* approximation corresponds well to the result of molecular dynamics simulation of −8.0 kcal/mol,[24] although it is substantially smaller than the value of stability of −16 kcal/mol obtained in another molecular dynamics simulation by Li Zhang and Hermans.[25] The apparent contribution of hydration thermodynamics to this preference that was found in our studies is significantly larger than the estimates from a molecular dynamics study.[24] Part of the difference could arise from differences in the empirical potentials that were employed. Differences in hydration energies from the MD calculations could be associated with the use of different potentials and different sampling techniques (e.g., see ref 18); however, MD sampling at least to some extent mimics the vibrational contribution to the free energy (or more precisely, the shape of the potential well) that is not accounted for in our quantum-chemical calculations. It is also known that the dipole moments obtained with 6-31G* basis sets are usually overestimated, thus leading to an overestimation of the hydration effects in our results.[40] On the other hand, according to the work of Li Zhang and Hermans,[25] the entropic contribution should favor the 3_{10} helix ($-T\Delta S^\circ = -4.0$ kcal/mol for decaalanine). Thus, entropic and hydration effects could work in different directions for the relative stability of α vs 3_{10} helices. We shall estimate possible errors due to both factors elsewhere.

From the entire conformational set that we studied, we singled out the central helix ($n = 8$) and analyze its isomeric forms in details here. The purpose of this focus is the elucidation of possible mechanisms of the conformational interconversion between the two helical forms. Our octapeptide results, computed in the gas phase at the HF/3-21G, HF/6-31G* and B3LYP/6-31G* levels of theory for HCO-NH-$(Ala)_8$-$CONH_2$ and in the aqueous solvent at B3LYP/6-31G* level of theory, are shown in Table 3. The comparison of the torsional angles optimized at the B3LYP/6-31G* level of theory to those obtained at the HF/3-21G level of theory (see Table 3) clearly indicated that the HF/3-21G-optimized torsional angles may be regarded to be at least semiquantitatively correct.

On the basis of lengths of the hydrogen bond in the conformations described in Table 3, one may ascertain the types of hydrogen bonds involved. These are shown graphically in Figure 2. For the 3_{10} helices, a full H bond is denoted by a solid line drawn from H to O (from top to bottom) along a direction corresponding to a line between 11 and 5 o'clock. For the 4_{13} helices (α helices) the full H bond is denoted by a heavy solid line drawn from H to O (from top to bottom) along a direction corresponding to a line between 1 and 7 o'clock. The hydrogen bond was considered to be full if the H-to-O separation was <2.4 Å. In such cases, the solid lines were applied in Figure 2. If the length of the H-to-O separation in the hydrogen bond fell within 2.4 to 2.6 Å, it was regarded as a partial hydrogen bond, and a broken line denoted it. H-to-O separations exceeding 2.6 Å were disregarded and are not marked as hydrogen bonds of any kind in Figure 2.

From Table 3 and Figures 2 we elucidate the following:

(i) If we disregard the hydrogen bond involving the formyl carbonyl oxygen because of the flexibility of the terminal formyl group, we find in the octapeptide ($n = 8$) six (i.e., n−2) hydrogen bonds for the 3_{10} helix and five (i.e., n−3) hydrogen bonds in the 4_{13} or α helix.

(ii) We may recognize two paths or two mechanisms for the $3_{10} \rightarrow 4_{13}$ interconversions as the H bonds flip over from the right to left, like an automobile windshield wiper. The first path starts the flip-over at the N- terminal (i.e. at the HCO-NH- end) and works its way toward the C- terminal (i.e., to the -$CONH_2$ end). The second path involves a change-over from the C-terminal and works its way toward the N- terminal. In other words, the starting point of the change in hydrogen bonding in the second path is opposite to that of the first path.

(iii) In the first path, we are able to locate two "reaction intermediates," that is, two partially converted helices. We denote these two structures as intermediate **I** and intermediate **I′**. In the second path, we are able to locate one partially converted helix that we denote as intermediate **II**. Figure 3 depicts the mechanistic relationship of these two paths. The energetics of these two interconversion pathways are shown in Figure 4.

(iv) It is important to note that the increase of the basis set size and the inclusion of electron correlation did make some quantitative difference in the computed results; however, for all computations carried out in the gas phase, the 3_{10} helix turned out to be the global minimum, and the 4_{13} or α helix appeared to be a local minimum, perhaps the highest of the local minimums. In contrast to these gas-phase results, when calculations included water, within the Poisson−Boltzmann model, the global minimum became the 4_{13} or α helix, and the highest local minimum appeared to be the 3_{10} helix.

(40) Rashin, A. A.; Young, L.; Topol, I. A. *Biophys. Chem.* **1994**, *51*, 359.

Table 3. Helical Structure Parameters for HCO-$(Ala)_8$-NH_2 Optimized at Different Levels of Theory in Two Media[a]

	3_{10} helix			intermediate I			intermediate II			α helix		
theory, medium	φ	ψ	ω	φ	ψ	ω	φ	ψ	ω	φ	ψ	ω
(1), HF/3-21G vacuum			−170.5			−172.3			−170.4	converged to intermediate I		
	−59.9	−29.8	−178.6	−57.1	−39.3	−176.5	−59.6	−29.7	−179.0			
	−58.9	−22.6	179.0	−61.5	−38.5	−179.7	−58.0	−24.2	179.1			
	−60.2	−22.3	178.4	−65.7	−42.6	177.5	−56.5	−32.4	−179.2			
	−60.5	−21.4	177.9	−58.6	−45.2	−179.1	−61.2	−38.6	179.6			
	−61.6	−20.2	177.5	−59.5	−42.1	−177.4	−72.2	−34.6	174.9			
	−62.3	−21.4	177.9	−58.9	−31.5	−179.7	−58.2	−37.2	−176.9			
	−73.0	−2.8	172.9	−68.5	−8.0	175.0	−83.4	−37.6	−164.4			
	−103.8	10.8	178.1	−101.0	8.9	178.4	−141.7	17.4	175.3			
(2), HF/6-31G* vacuum			−167.1						−167.0			
	−66.0	−25.4	−178.8				−66.1	−24.9	−179.3			
	−62.9	−21.5	179.1				−62.7	−21.5	179.1			
	−63.7	−19.3	178.9				−60.3	−27.9	−179.8			
	−61.2	−23.9	179.0				−64.1	−33.7	177.1			
	−62.6	−23.3	179.3				−73.5	−38.6	179.7			
	−68.6	−15.0	178.2				−66.3	−28.3	−176.9			
	−67.7	−15.7	176.4				−67.4	−18.4	178.7			
	−83.5	−7.3	175.3				−84.6	−7.4	176.3			
(3), DFT/B3LYP6-31G* vacuum			−167.5			−170.1			−167.2			−170.7
	−63.8	−25.5	177.9	−60.6	−34.1	−180.0	−63.2	−26.0	177.9	−60.2	−34.8	179.7
	−60.2	−21.1	176.6	−65.9	−33.6	176.2	−58.9	−22.9	177.6	−65.7	−32.9	176.5
	−62.2	−17.0	174.4	−69.6	−38.2	175.6	−58.0	−28.1	177.7	−69.6	−38.9	174.5
	−57.8	−24.6	176.8	−61.8	−41.1	177.8	−64.7	−36.5	176.4	−60.9	−41.8	177.8
	−60.5	−23.0	177.3	−65.4	−41.7	−179.4	−74.0	−33.5	175.7	−62.8	−41.9	178.5
	−65.4	−17.4	175.3	−62.3	−29.8	179.4	−65.9	−32.9	−175.6	−64.6	−35.4	178.1
	−70.0	−7.9	172.4	−68.2	−10.1	174.2	−92.6	−27.9	−171.3	−75.9	−25.7	−174.3
	−98.4	6.6	176.7	−98.9	7.0	179.1	−132.2	5.7	178.4	−112.0	3.7	−174.5
(4), DFT/B3LYP6-31G* water			−172.7			−173.9			−172.8			−174.2
	−59.3	−28.2	179.4	−57.5	−38.5	−178.6	−59.6	−27.8	178.7	−57.2	−37.7	−178.9
	−56.5	−24.9	178.9	−63.9	−35.5	177.8	−56.6	−24.3	177.6	−63.3	−35.3	177.3
	−59.2	−22.7	177.2	−70.0	−40.0	175.6	−56.7	−30.7	178.2	−69.4	−38.4	174.0
	−58.2	−25.3	177.5	−61.6	−43.0	178.1	−67.2	−34.6	174.4	−62.7	−41.3	177.7
	−61.1	−21.8	175.5	−63.9	−47.3	−179.0	−72.4	−36.5	174.9	−64.7	−41.4	177.3
	−60.2	−24.8	176.5	−60.8	−36.9	179.6	−62.0	−39.1	−177.7	−64.2	−39.8	177.8
	−65.8	−15.1	174.8	−64.5	−18.0	175.4	−78.0	−40.2	−165.7	−65.9	−37.9	179.6
	−95.2	4.7	178.6	−94.2	1.2	179.1	−135.1	8.3	−179.3	−72.4	−31.8	−175.5

	Energy, a.u.			
(1), HF/3-21G vacuum	−2123.9245576	−2123.9224861[b]	−2123.9161236	
(2), HF/6-31G* vacuum	−2135.7811739		−2135.7764130	
(3), DFT/B3LYP6-31G* vacuum	−2148.5405101	−2148.5329400	−2148.5330143	−2148.5301617
(4), DFT/B3LYP6-31G* water	−2148.7077673	−2148.7212521	−2148.7201031	−2148.7315778
	Relative Energy, kcal/mol			
(1), HF/3-21G vacuum	0.00	1.30[b]	5.29	
(2), HF/6-31G* vacuum	0.00	2.99		
(3), DFT/B3LYP6-31G* vacuum	0.00	4.75	4.70	6.49
(4), DFT/B3LYP6-31G* water	0.00	−8.46	−7.74	−14.94

[a] Each line represents dihedral angles of one residue in up to four conformations. First line for each of "theory/media" groups corresponds to HCO terminal group. [b] Intermediate I′.

Our results and their agreement with the conclusions of some experimental studies have an important bearing on our understanding of the protein-folding process. If, as our calculations suggest, the α helices tend to be the thermodynamically preferred helical conformation in solution, then the folding of the tertiary structure might proceed from helices "prefabricated" as the pieces of the secondary structure at the early stages of the folding process. If, however, the conclusions from other experiments[16] are correct, it might be that the pieces of the secondary structure could be significantly changed when they form the tertiary contacts. The latter possibility would make the folding process as well as its prediction more complicated. Although the side-chain influences could override any of the preferences found for polyalanine helices, further study of the factors contributing to the α-to-3_{10}-helix interconversion seem to be warranted.

4. Conclusions

This paper presents the first ab initio and DFT calculations performed for the helical polyalanine structures longer than one helical turn in the gas phase and in aqueous solvent. Choosing the helical structure for the test, we found that the intrinsic

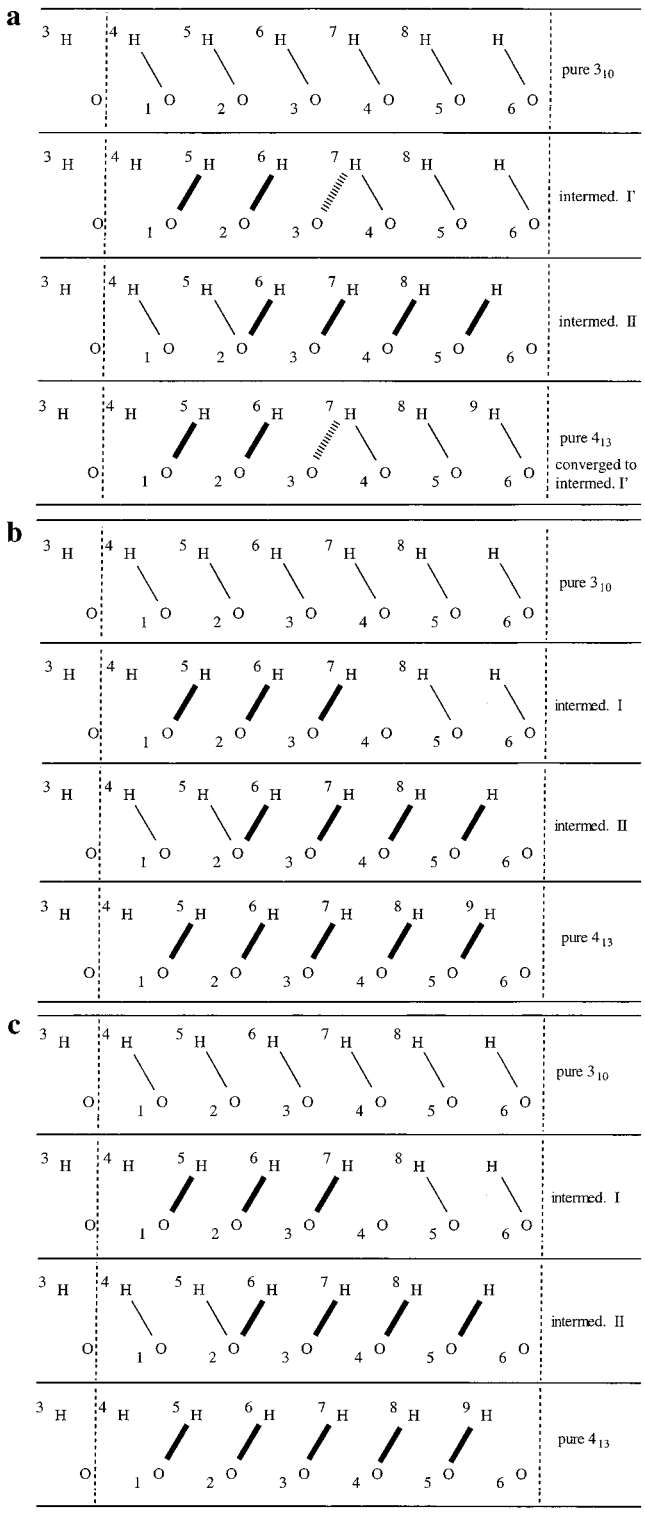

Figure 2. Hydrogen bonding pattern in HCO-$(Ala)_8$-NH_2 optimized at different levels of theory: (a) HF/3-21G in the gas phase; (b) B3LYP/6-31G* in the gas phase; (c) B3LYP/6-31G* in water. The unnumbered oxygen atom at the left-hand side is the terminal formyl oxygen and the numbered hydrogen atom at the right-hand side is associated with the terminal -NH_2 group. Hydrogen bonds are shown by a "slash" for 3_{10}, a "backslash" for 4_{13}, a solid line for an O···H interatomic distance lower than 2.4 Å, and a broken line for 2.4−2.6 Å.

properties (e.g., torsional angles) obtained at the B3LYP/6-31G* level of theory were reproduced at least semiquantitatively at the HF/3-21G level. This level of approximation could be successfully used in further studies of much larger polypeptides.

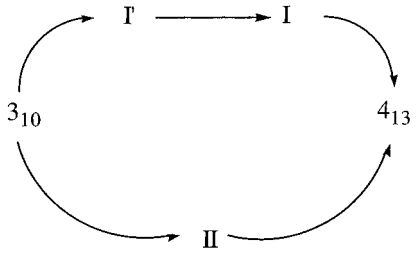

Figure 3. The mechanistic relationship of the two paths of $3_{10} \rightarrow 4_{13}$ helix interconversion for HCO-$(Ala)_8$-NH_2. In the first path, we locate two "reaction intermediates," that is, two partially converted helices. These two structures are denoted as intermediate **I′** and intermediate **I**. In the second path, we located one partially converted helix that is denoted as intermediate **II**. The energetics of these two interconversion pathways are shown in Figure 4.

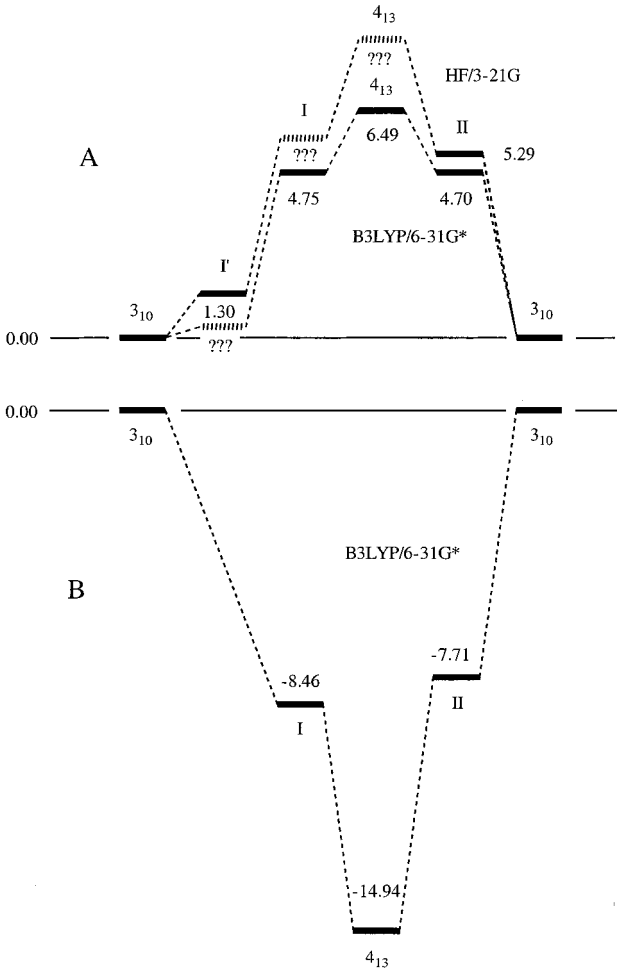

Figure 4. Energy profile of the $3_{10} \rightarrow 4_{13}$ helical interconversions. Only reactant, product, and intermediates are shown in the energy-level diagram. Hypothetical conformers not found in the present work are represented by interrupted lines and question marks. A, gas phase; B, aqueous solvent.

All three approximations (HF/3-21G, HF/6-31G*, and B3LYP/6-31G*) predicted the 3_{10} helix to be the global minimum in the gas phase. Only when solvation effects were included within the Poisson−Boltzmann approximation at the B3LYP/6-31G* level of theory, did the 4_{13} or α helix became substantially more stable than the 3_{10} helix.

Our calculations revealed that there may be more than one mechanism for the $3_{10} \rightarrow 4_{13}$ interconversion. We identified two paths or two mechanisms for the $3_{10} \rightarrow 4_{13}$ interconversions as the H bonds flip over. The first path starts the flip-over at the

N- terminal (i.e., at the HCO-NH- end) and works its way toward the C- terminal (i.e., to the -$CONH_2$ end). The second path involves a change-over from the C- terminal and works its way toward the N- terminal. The calculation results regarding changes of terminal subunit structures correspond well with recent solid-state and solution NMR data.[21,22]

Understanding of the α-to-3_{10}-helix interconversion and equilibrium can be important for the theory of protein folding and for the protein structure predictions.

Acknowledgment. The authors thank the staff and administration of the ABCC for their support of this project. This project has been funded in part with Federal funds from the National Cancer Institute, National Institutes of Health, under Contract No. NO1-CO-56000. This project also was supported in part by grants from the Hungarian Scientific Research Fund (OTKA T024044, T032486). The content of this publication does not necessarily reflect the views or policies of the Department of Health and Human Services, nor does mention of trade names, commercial products, or organization imply endorsement by the U.S. Government.

JA0038934